User Scheduling and Passive Beamforming for FDMA/OFDMA in Intelligent Reflection Surface

Wei Jiang[*†] and Hans D. Schotten[†*]

[*]Intelligent Networking Research Group, German Research Center for Artificial Intelligence (DFKI)

[†]Department of Electrical and Computer Engineering, Technische Universität (TU) Kaiserslautern

Abstract

Most prior works on intelligent reflecting surface (IRS) merely consider point-to-point communications, including a single user, for ease of analysis. Nevertheless, a practical wireless system needs to accommodate multiple users simultaneously. Due to the lack of frequency-selective reflection, namely the set of phase shifts cannot be different across frequency subchannels, the integration of IRS imposes a fundamental challenge to frequency-multiplexing approaches such as frequency-division multiple access (FDMA) and the widely adopted technique called orthogonal FDMA (OFDMA). It motivates us to study (O)FDMA-based multi-user IRS communications to clarify which user scheduling and passive beamforming are favorable under this non-frequency-selective reflection environment. Theoretical analysis and numerical evaluation reveal that (O)FDMA does not need user scheduling when there are a few users. If the number of users becomes large, neither user scheduling nor IRS reflection optimization is necessary. These findings help substantially simplify the design of (O)FDMA-based IRS communications.

I. INTRODUCTION

Motivated by the big commercial success of the fourth generation a.k.a 3GPP LTE-Adavnced [1]–[3] and the fifth generation (5G) technology [4]–[14], both the academia and industry have already shifted their focus towards the sixth generation (6G) [15]–[18] and enthusiastically initiated many pioneering research programs although 5G is still on its way to being deployed across the world. To support disruptive use cases beyond 2030, such as holographic communications, extended reality, artificial intelligence [19]–[28], Tactile Internet, Internet of Things [29]–[35], multi-sense experience, metaverse, digital twin, and block-chain [36], 6G needs to meet more stringent performance requirements than its predecessor, e.g., a peak data rate of 1 terabits-per-second (Tbps), a missive connection density of 10^7 devices per km^2, and high-accuracy positioning, sensing [37]–[39], identification and tracking [40]–[42]. Traditionally, three major approaches, i.e., *(1) Deploying Dense and Heterogeneous Networks*, *(2) Installing Massive Antennas for Extreme Spectral Efficiency*, and *(3) Enlarging Bandwidth* can effectively improve coverage and capacity. Nevertheless, these approaches incur high capital and operational expenditures, unaffordable energy consumption, and severe network interference. Given these limitations, further evolving along the old track is hard to fully achieve stringent 6G requirements. Therefore, it is highly desirable to develop a revolutionary technology to realize sustainable capacity and performance growth with affordable cost, low complexity, and efficient energy consumption.

Along with other 6G-potential technologies, such as terahertz communications [43]–[45] and cell-free massive MIMO [46]–[51], a disruptive technique referred to as intelligent reflecting surface (IRS), a.k.a. reconfigurable intelligent surface, has drawn much attention from academia and industry because of its potential of reaping high performance in a green and cost-effective way [52]–[57]. Particularly, IRS is a planar meta-surface consisting of a large number of passive, lightweight, and cheap reflection elements. A smart controller dynamically adjusts the phase shift of each element, thereby collaboratively achieving

smart propagation environment for signal amplification or interference suppression [58]. Conventional technologies, such as *dense and heterogeneous network deployment*, *massive antennas*, and *ultra-wide bandwidth*, can improve coverage and capacity effectively but incur high capital and operational expenditures, much energy consumption, and severe network interference. In contrast, IRS not only reflects signals in a full-duplex and noise-free way [59] but also lowers hardware and energy costs substantially thanks to the use of passive components. Consequently, it is widely recognized that IRS can serve as a key technological enabler for the upcoming sixth-generation (6G) wireless system to meet more stringent performance requirements than its predecessor [16].

Previous studies have investigated different aspects for IRS-aided wireless communications, e.g., passive beamforming [58], reflected channel estimation [60], hardware constraints [61], and the interplay with other technologies, such as orthogonal frequency-division multiplexing (OFDM) [62], multi-input multi-output (MIMO) [63], hybrid beamforming [64], and Terahertz communications [45]. The majority of prior works focus on point-to-point IRS-aided communications, which merely considers a single user for simplicity. Nevertheless, a practical system needs to accommodate many users simultaneously, especially in scenarios such as massive connectivity, raising the problem of multiple access. Usually, the phase shift of an element is adaptively tuned across different time instants (i.e., time-selective). Due to the hardware constraint, it is not frequency-selective, namely the phase shift cannot be different across frequency subchannels. Hence, the integration of IRS imposes a fundamental challenge to frequency-multiplexing approaches such as frequency-division multiple access (FDMA), including the widely adopted technique called orthogonal FDMA (OFDMA) [65].

In [66], the authors revealed that non-orthogonal multiple access (NOMA) and time-division multiple access (TDMA) are superior to FDMA in terms of spectral efficiency. However, NOMA needs complex signal processing for successive interference cancellation (SIC) [67], while TDMA requires stringent time synchronization among users. It is envisioned that FDMA can still play an important role in some particular 6G scenarios such as IRS-assisted Internet of Things [68] due to its simple implementation. Meanwhile, intelligent surfaces can be transparently installed in legacy FDMA-based networks for performance enhancement, especially for OFDMA-empowered 4G LTE and 5G NR. Hence, it is worth making clear the behaviours of (O)FDMA-based multi-user IRS systems in the absence of frequency-selective reflection, which is not reported yet in the literature to the best knowledge of the authors. For simplicity, we use FDMA hereinafter to represent both legacy FDMA and OFDMA techniques.

Since the IRS in FDMA-based systems can only be optimized for a particular user/subchannel, it raises two fundamental questions: i) which user should be selected for optimizing passive beamforming? and ii) how to optimize the passive beamforming? In this paper, therefore, we investigate the effects of multi-user scheduling and reflection optimization in an IRS-aided FDMA system (interchangeably using the term *FDMA-IRS* hereinafter). Spectral efficiency for different user-scheduling and passive-beamforming strategies are analytically derived, while a simulation setup consisting of a cell-edge area and a cell-center area is deliberately designed to compare their performance with TDMA and power-domain NOMA. Theoretical analysis and numerical evaluation reveal a meaningful outcome. That is, FDMA-IRS does not need user scheduling when there are a few users. If the number of users becomes large, *neither* user scheduling *nor* passive-beamforming optimization is necessary. This findings helps substantially simplifying the design of FDMA-IRS, where at least the estimation of cascaded channels, the IRS tuning, the smart controller, and its backhaul are not needed any more.

We organize the rest of this paper as follows: Section II gives the system model. Section III analyzes user scheduling and reflection optimization for FDMA-based IRS communications. Simulation setup and some examples of numerical results are demonstrated in Section IV. Finally, Section V summarizes this paper.

II. System Model

As illustrated in Fig.1, this paper focuses on the downlink of an IRS-assisted multi-user MIMO system, where an intelligent surface with N reflecting elements is deployed to aid the transmission from an N_b-antenna BS to K single-antenna user equipment (UE). We write

$$\mathbf{f}_k = \left[f_{k1}, f_{k2}, \ldots, f_{kN_b} \right]^T \tag{1}$$

to denote the $N_b \times 1$ channel vector between the BS and the kth UE, and

$$\mathbf{g}_k = \left[g_{k1}, g_{k2}, \ldots, g_{kN} \right]^T \tag{2}$$

to denote the $N \times 1$ channel vector between the IRS and UE k. Denoting the channel vector from the BS to the nth reflecting element by $\mathbf{h}_n = [h_{n1}, h_{n2}, \ldots, h_{nN_b}]^T$, the channel matrix from the BS to the IRS is expressed as $\mathbf{H} \in \mathbb{C}^{N \times N_b}$, where the nth row of $\mathbf{H}$ equals to $\mathbf{h}_n^T$. Since the line-of-sight (LOS) paths from either the BS or the IRS to UEs may be blocked, the corresponding small-scale fading follows Rayleigh distribution. Consequently, f and g are circularly symmetric complex Gaussian random variables denoted by $f \sim \mathcal{CN}(0, \sigma_f^2)$ and $g \sim \mathcal{CN}(0, \sigma_g^2)$, respectively. In contrast, a favourable location is deliberately selected for the IRS to exploit an LOS path to the fixed BS without any blockage, resulting in Rician fading, i.e.,

$$\mathbf{H} = \sqrt{\frac{\Gamma \sigma_h^2}{\Gamma + 1}} \mathbf{H}_{LOS} + \sqrt{\frac{\sigma_h^2}{\Gamma + 1}} \mathbf{H}_{NLOS} \tag{3}$$

with the Rician factor Γ, the LOS component $\mathbf{H}_{LOS}$, the multipath component $\mathbf{H}_{NLOS}$ consisting of independent entries that follow $\mathcal{CN}(0, 1)$, and the BS-IRS path loss σ_h^2.

Since the IRS is a passive device, time-division duplexing (TDD) operation is usually adopted to simplify channel estimation. The users send pilot signals in the uplink training and the BS estimates the uplink instantaneous channel state information (CSI), which is used for optimizing downlink data transmission due to channel reciprocity. To characterize the theoretical performance, the analysis is conducted under the assumption that the BS perfectly knows the CSI of all involved channels, as most prior works [52], [58], [59]. Moreover, we do not consider the impact of channel aging or outdated channel information in fast-fading environments [69]–[77]. A wideband channel suffering from frequency selectivity can be transformed into a set of narrowband channels through OFDM [65], [78]–[83], and therefore we can conduct the algorithm design over a frequency-flat narrowband subcarrier. A smart controller adaptively adjusts the phase shift of each reflecting element based on the instantaneous CSI acquired through periodic channel estimation [60]. The reflection of a typical element n is mathematically modeled by a coefficient $\epsilon_n = a_n e^{j\phi_n}$, where $\phi_n \in [0, 2\pi)$ denotes an induced phase shift, and $a_n \in [0, 1]$ stands for amplitude attenuation. As mentioned by [58], $a_n = 1, \forall n$ is the optimal attenuation that maximizes the strength of the received signal and simplifies the implementation complexity. Hence, the reflection optimization only focuses on the phase shifts $\phi_n, \forall n$. By ignoring hardware impairments such as quantified phase shifts [84] and phase noise [55], the kth UE observes the received signal

$$r_k = \sqrt{P_t} \left(\sum_{n=1}^{N} g_{kn} e^{j\phi_n} \mathbf{h}_n^T + \mathbf{f}_k^T \right) \mathbf{s} + n_k, \tag{4}$$

where $\mathbf{s}$ denotes the vector of transmitted signals over the BS antenna array, P_t expresses the transmit power, n_k is additive white Gaussian noise (AWGN) with zero mean and variance σ_n^2, namely $n_k \sim \mathcal{CN}(0, \sigma_n^2)$. Define

$$\mathbf{\Theta}_0 = \mathrm{diag}\left\{ e^{j\phi_1}, e^{j\phi_2}, \ldots, e^{j\phi_N} \right\}, \tag{5}$$

(4) can be rewritten in matrix form as

$$r_k = \sqrt{P_t} \left(\mathbf{g}_k^T \mathbf{\Theta}_0 \mathbf{H} + \mathbf{f}_k^T \right) \mathbf{s} + n_k. \tag{6}$$
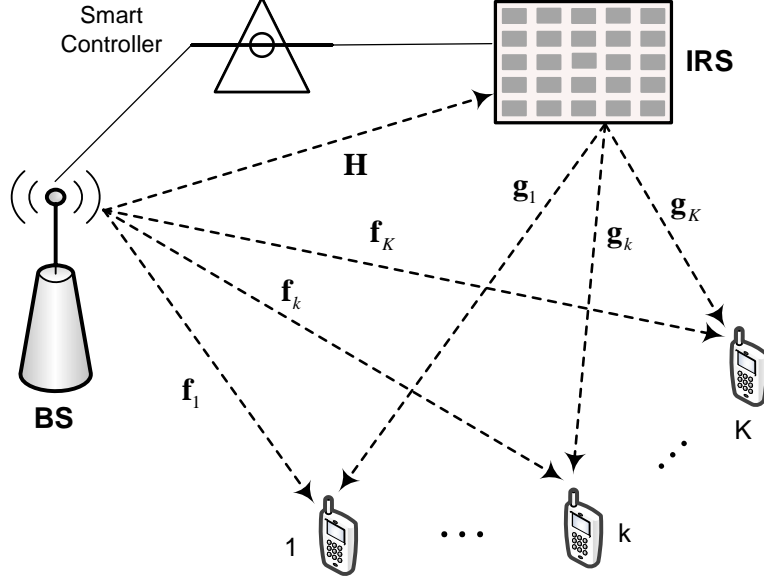
Fig. 1. Schematic diagram of an IRS-aided multi-user MIMO system, consisting of a multi-antenna BS, K single-antenna UE, and a reflecting surface with N IRS elements.

III. USER SCHEDULING AND OPTIMIZATION DESIGN

The fundamental of FDMA lies on the division of the whole system bandwidth into K orthogonal subchannels. Each user occupies a dedicated subchannel over the entire time. At the kth subchannel, the BS can employ linear beamforming [85]–[91] over the antenna array denoted by $\mathbf{w}_k \in \mathbb{C}^{N_b \times 1}$, where $\|\mathbf{w}_k\|^2 \leqslant 1$, to send the information symbol s_k intended for user k, which satisfies $\mathbb{E}\left[|s_k|^2\right] = 1$. For simplicity, the transmit power of the BS is equally allocated among subchannels, i.e., $P_t = P_d/K$, where P_d expresses the power constraint of the BS.

Substituting $\mathbf{s} = \mathbf{w}_k s_k$ and $P_t = P_d/K$ into (6), we obtain

$$r_k = \sqrt{\frac{P_d}{K}}\left(\mathbf{g}_k^T \boldsymbol{\Theta}_0 \mathbf{H} + \mathbf{f}_k^T\right)\mathbf{w}_k s_k + n_k. \tag{7}$$

Thus, the achievable spectral efficiency of user k is formulated as

$$R_k = \frac{1}{K}\log\left(1 + \frac{\frac{P_d}{K}\left|\left(\mathbf{g}_k^T \boldsymbol{\Theta}_0 \mathbf{H} + \mathbf{f}_k^T\right)\mathbf{w}_k\right|^2}{\frac{\sigma_n^2}{K}}\right), \tag{8}$$

where the factor $1/K$ is applied since the signal transmission of each user occupies only $1/K$ of the total bandwidth. As a result, the sum rate of the IRS-aided FDMA system is

$$C = \sum_{k=1}^{K} \frac{1}{K}\log\left(1 + \frac{P_d\left|\left(\mathbf{g}_k^T \boldsymbol{\Theta}_0 \mathbf{H} + \mathbf{f}_k^T\right)\mathbf{w}_k\right|^2}{\sigma_n^2}\right). \tag{9}$$

A. Multi-User Scheduling

Unlike an IRS-aided TDMA system, where the set of phase shifts at each slot can be dynamically adjusted for its assigned user, the IRS in an FDMA system can be optimized only for a particular user $\hat{k}$ by setting $\boldsymbol{\Theta}_{\hat{k}}$. The remaining users $k \neq \hat{k}$

over other subchannels have to utilize this common configuration with $\boldsymbol{\Theta}_{\hat{k}}$ and suffer from phase-unaligned reflection. That is because the hardware constraint of IRS elements, which can be tuned in *time-selective* but not *frequency-selective*. Hence, it raises a particular issue of *user scheduling* in FDMA: which user should be selected for passive beamforming optimization? To get a comprehensive view, we design the following strategies:

- *Exhaustive Search:* If the system applies the IRS to aid the signal transmission of a typical user k, the set of phase shifts is adjusted according to the CSI of this user, i.e., $\boldsymbol{\Theta}_0 = f(\mathbf{f}_k, \mathbf{g}_k, \mathbf{H})$, where $f(\cdot)$ denotes a certain optimization function. In this case, the achievable sum rate denoted by $C(k)$ can be computed by (9). The best user selection, which achieves the maximal sum rate, is determined by exhaustively setting each user as the IRS-aided user

$$\hat{k} = \arg\max_{k \in \mathcal{K}} C(k), \tag{10}$$

  where $\mathcal{K} = \{1, 2, \ldots, K\}$ represents the set of users.

- *The Nearest User:* The philosophy behind is that the system performance might be improved by applying the IRS to aid the user that has the smallest distance (equivalent to the largest large-scale fading or average received power) to the IRS. Without losing generality, the user is selected according to

$$\hat{k} = \arg\max_{k \in \mathcal{K}} \mathbb{E}\left[\|\mathbf{g}_k\|^2\right], \tag{11}$$

  where $\|\cdot\|$ expresses the Frobenius norm, and $\mathbb{E}$ denotes the statistical expectation.

- *The Farthest User:* For comparison, we can also optimize the phase shifts for the user that has the largest distance to the IRS, i.e.,

$$\hat{k} = \arg\min_{k \in \mathcal{K}} \mathbb{E}\left[\|\mathbf{g}_k\|^2\right]. \tag{12}$$

- *Random Selection* where the IRS adjusts its phase shifts according to the CSI of a user that is randomly selected from $\mathcal{K}$. In other words, the IRS is optimized as $\boldsymbol{\Theta}_0 = f(\mathbf{f}_k, \mathbf{g}_k, \mathbf{H})$ given a random user k. Note that random user selection differs from random IRS reflection, where the phase shifts are random without optimization, independent of the CSI of any user.

B. Joint Reflection Optimization

When the best user $\hat{k}$ is determined through user scheduling, the system needs the joint optimization of active beamforming at the BS and passive reflection at the IRS to aid the signal transmission of $\hat{k}$. Temporarily ignoring other users $k \neq \hat{k}$, the closed-form solutions for optimal active beamforming and optimal reflection can be obtained through an alternating method as presented below. To maximize the instantaneous signal-to-noise ratio (SNR) of user $\hat{k}$, i.e.,

$$\gamma_{\hat{k}} = \frac{P_d \left|(\mathbf{g}_{\hat{k}}^T \boldsymbol{\Theta}_0 \mathbf{H} + \mathbf{f}_{\hat{k}}^T) \mathbf{w}_{\hat{k}}\right|^2}{\sigma_n^2}, \tag{13}$$

we formulate the following optimization problem

$$\max_{\boldsymbol{\Theta}_0, \mathbf{w}_{\hat{k}}} \left|\left(\mathbf{g}_{\hat{k}}^T \boldsymbol{\Theta}_0 \mathbf{H} + \mathbf{f}_{\hat{k}}^T\right) \mathbf{w}_{\hat{k}}\right|^2$$
$$\text{s.t.} \quad \|\mathbf{w}_{\hat{k}}\|^2 \leqslant 1 \tag{14}$$
$$\phi_n \in [0, 2\pi), \ \forall n = 1, 2, \ldots, N,$$

which is non-convex because their objective function is not jointly concave with respect to $\boldsymbol{\Theta}_0$ and $\mathbf{w}_{\hat{k}}$. To solve this problem, we can alternately optimize $\boldsymbol{\Theta}_0$ and $\mathbf{w}_{\hat{k}}$ in an iterative manner [58].

Without loss of generality, the maximal-ratio transmission (MRT) for the direct link can be applied as the initial value of the transmit vector, i.e., $\mathbf{w}_{\hat{k}}^{(0)} = \mathbf{f}_{\hat{k}}^* / \|\mathbf{f}_{\hat{k}}\|$. Thus, (14) is simplified to

$$\max_{\boldsymbol{\Theta}_0} \quad \left| \left(\mathbf{g}_{\hat{k}}^T \boldsymbol{\Theta}_0 \mathbf{H} + \mathbf{f}_{\hat{k}}^T \right) \mathbf{w}_{\hat{k}}^{(0)} \right|^2$$

$$\text{s.t.} \quad \phi_n \in [0, 2\pi), \ \forall n = 1, 2, \dots, N. \tag{15}$$

The objective function is still non-convex but it enables a closed-form solution through applying the well-known triangle inequality

$$\left| \left(\mathbf{g}_{\hat{k}}^T \boldsymbol{\Theta}_0 \mathbf{H} + \mathbf{f}_{\hat{k}}^T \right) \mathbf{w}_{\hat{k}}^{(0)} \right| \leqslant \left| \mathbf{g}_{\hat{k}}^T \boldsymbol{\Theta}_0 \mathbf{H} \mathbf{w}_{\hat{k}}^{(0)} \right| + \left| \mathbf{f}_{\hat{k}}^T \mathbf{w}_{\hat{k}}^{(0)} \right|. \tag{16}$$

The equality achieves if and only if

$$\arg\left(\mathbf{g}_{\hat{k}}^T \boldsymbol{\Theta}_0 \mathbf{H} \mathbf{w}_{\hat{k}}^{(0)} \right) = \arg\left(\mathbf{f}_{\hat{k}}^T \mathbf{w}_{\hat{k}}^{(0)} \right) \triangleq \varphi_0, \tag{17}$$

where $\arg(\cdot)$ stands for the component-wise phase of a complex vector.

Define $\mathbf{b}_0 = [b_1, b_2, \dots, b_N]^H$ with $b_n = e^{j\phi_n}$ and $\boldsymbol{\chi}_{\hat{k}} = \text{diag}(\mathbf{g}_{\hat{k}}^T) \mathbf{H} \mathbf{w}_{\hat{k}}^{(0)} \in \mathbb{C}^{N \times 1}$, we have $\mathbf{g}_{\hat{k}}^T \boldsymbol{\Theta}_0 \mathbf{H} \mathbf{w}_{\hat{k}}^{(0)} = \mathbf{b}_0^H \boldsymbol{\chi}_{\hat{k}} \in \mathbb{C}$. Ignore the constant term $\left| \mathbf{f}_{\hat{k}}^T \mathbf{w}_{\hat{k}}^{(0)} \right|$, (15) is transformed to

$$\max_{\mathbf{b_0}} \quad \left| \mathbf{b}_0^H \boldsymbol{\chi}_{\hat{k}} \right|$$

$$\text{s.t.} \quad |b_n| = 1, \ \forall n = 1, 2, \dots, N, \tag{18}$$

$$\arg(\mathbf{b}_0^H \boldsymbol{\chi}_{\hat{k}}) = \varphi_0.$$

The solution for (18) can be derived as

$$\mathbf{b}_0^{(1)} = e^{j\left(\varphi_0 - \arg(\boldsymbol{\chi}_{\hat{k}}) \right)} = e^{j\left(\varphi_0 - \arg\left(\text{diag}(\mathbf{g}_{\hat{k}}^T) \mathbf{H} \mathbf{w}_{\hat{k}}^{(0)} \right) \right)}. \tag{19}$$

Equivalently,

$$\phi_n^{(1)} = \varphi_0 - \arg\left(g_{\hat{k}n} \mathbf{h}_n^T \mathbf{w}_{\hat{k}}^{(0)} \right)$$

$$= \varphi_0 - \arg\left(g_{\hat{k}n} \right) - \arg\left(\mathbf{h}_n^T \mathbf{w}_{\hat{k}}^{(0)} \right), \tag{20}$$

where $\mathbf{h}_n^T \mathbf{w}_{\hat{k}}^{(0)} \in \mathbb{C}$ can be regarded as an effective SISO channel perceived by the nth reflecting element, combining the effects of transmit beamforming $\mathbf{w}_{\hat{k}}^{(0)}$ and channel response $\mathbf{h}_n$. In this regard, (20) implies that an IRS reflector should be tuned such that the residual phase of each reflected signal is aligned with the phase of the signal over the direct link for coherent combining at the receiver.

Once the phase shifts at the first iteration, i.e., $\boldsymbol{\Theta}_0^{(1)} = \text{diag}\left\{ e^{j\phi_1^{(1)}}, e^{j\phi_2^{(1)}}, \dots, e^{j\phi_N^{(1)}} \right\}$ are determined, the optimization is alternated to update $\mathbf{w}_{\hat{k}}$. The BS applies MRT a.k.a. matched filtering to maximize the strength of the desired signal, resulting in

$$\mathbf{w}_{\hat{k}}^{(1)} = \frac{\left(\mathbf{g}_{\hat{k}}^T \boldsymbol{\Theta}_0^{(1)} \mathbf{H} + \mathbf{f}_{\hat{k}}^T \right)^H}{\left\| \mathbf{g}_{\hat{k}}^T \boldsymbol{\Theta}_0^{(1)} \mathbf{H} + \mathbf{f}_{\hat{k}}^T \right\|}. \tag{21}$$

After the completion of the first iteration, the BS gets $\boldsymbol{\Theta}_0^{(1)}$ and $\mathbf{w}_{\hat{k}}^{(1)}$, which serve as the initial input for the second iteration to derive $\boldsymbol{\Theta}_0^{(2)}$ and $\mathbf{w}_{\hat{k}}^{(2)}$. This process iterates until the convergence is achieved with the optimal beamformer $\mathbf{w}_{\hat{k}}^{\star}$ and optimal reflection $\boldsymbol{\Theta}_0^{\star}$. Here, the convergence means the objective value of (14) is non-increasing over iterations, which can be implemented flexibly.

Applying $\mathbf{w}_{\hat{k}}^{\star}$ and $\boldsymbol{\Theta}_0^{\star}$ into (13), we derive the achievable spectral efficiency of user $\hat{k}$ as

$$R_{\hat{k}} = \frac{1}{K} \log \left(1 + \frac{P_d \left| \left(\mathbf{g}_{\hat{k}}^T \boldsymbol{\Theta}_0^{\star} \mathbf{H} + \mathbf{f}_{\hat{k}}^T \right) \mathbf{w}_{\hat{k}}^{\star} \right|^2}{\sigma_n^2} \right). \tag{22}$$

Given the reflection $\boldsymbol{\Theta}_0^{\star}$, what the remaining $K-1$ users can do is to achieve partial optimization (in contrast to the joint optimization for user $\hat{k}$) by updating their respective active beamforming. The MRT beamformer for user $k \neq \hat{k}, \forall k = 1, 2, \ldots, K$ is optimized as

$$\mathbf{w}_k^{\star} = \frac{\left(\mathbf{g}_k^T \boldsymbol{\Theta}_0^{\star} \mathbf{H} + \mathbf{f}_k^T \right)^H}{\left\| \mathbf{g}_k^T \boldsymbol{\Theta}_0^{\star} \mathbf{H} + \mathbf{f}_k^T \right\|}. \tag{23}$$

Substituting the optimal parameters into (9), the sum rate of the FDMA IRS system is obtained as

$$C = \underbrace{\frac{1}{K} \log \left(1 + \frac{P_d \left| \left(\mathbf{g}_{\hat{k}}^T \boldsymbol{\Theta}_0^{\star} \mathbf{H} + \mathbf{f}_{\hat{k}}^T \right) \mathbf{w}_{\hat{k}}^{\star} \right|^2}{\sigma_n^2} \right)}_{\text{Joint-Optimized User}} \tag{24}$$

$$+ \underbrace{\sum_{k=1, k \neq \hat{k}}^{K} \frac{1}{K} \log \left(1 + \frac{P_d \left| \left(\mathbf{g}_k^T \boldsymbol{\Theta}_0^{\star} \mathbf{H} + \mathbf{f}_k^T \right) \mathbf{w}_k^{\star} \right|^2}{\sigma_n^2} \right)}_{\text{Partial-Optimized Users}}$$

$$= \frac{1}{K} \log \left(1 + \left\| \mathbf{g}_{\hat{k}}^T \boldsymbol{\Theta}_0^{\star} \mathbf{H} + \mathbf{f}_{\hat{k}}^T \right\|^2 \frac{P_d}{\sigma_n^2} \right)$$

$$+ \sum_{k=1, k \neq \hat{k}}^{K} \frac{1}{K} \log \left(1 + \left\| \mathbf{g}_k^T \boldsymbol{\Theta}_0^{\star} \mathbf{H} + \mathbf{f}_k^T \right\|^2 \frac{P_d}{\sigma_z^2} \right).$$

C. Random Reflection

In addition to the joint optimization of passive reflection and active beamforming, we study the simplest solution as a baseline. Randomly setting the phase shifts of IRS elements denoted by $\boldsymbol{\Theta}_r$, each entry of which takes value uniformly and randomly from $[0, 2\pi)$. Then, each subchannel just optimizes its transmit beamforming as

$$\mathbf{w}_k^{\star} = \frac{\left(\mathbf{g}_k^T \boldsymbol{\Theta}_r \mathbf{H} + \mathbf{f}_k^T \right)^H}{\left\| \mathbf{g}_k^T \boldsymbol{\Theta}_r \mathbf{H} + \mathbf{f}_k^T \right\|}. \tag{25}$$

Since the phase shifts are random without the knowledge of CSI, the channel estimation of cascaded channels is avoided, substantially simplifying the system complexity.

IV. PERFORMANCE EVALUATION

In this section, we illustrate some numerical results of achievable spectral efficiency to compare the performance of FDMA, TDMA and NOMA. Different user scheduling and reflection optimization strategies for FDMA are evaluated. As shown in Fig.2, we consider the cell coverage consisting of a cell-center area and a cell-edge area. The BS equipped with $N_b = 16$ antennas is located at the original point $(0, 0)$ of the coordinate system, while a surface containing $N = 200$ reflecting elements is installed at the center of the cell-edge area, with the coordinate $(375\text{m}, 375\text{m})$. Half of the users are far users that distribute randomly over the cell-edge area, while the other half of users are near users that distribute randomly over the cell-edge area. The maximum transmit power of BS is $P_d = 20\text{W}$ over a signal bandwidth of $B_w = 20\text{MHz}$, referring to the practical 3GPP
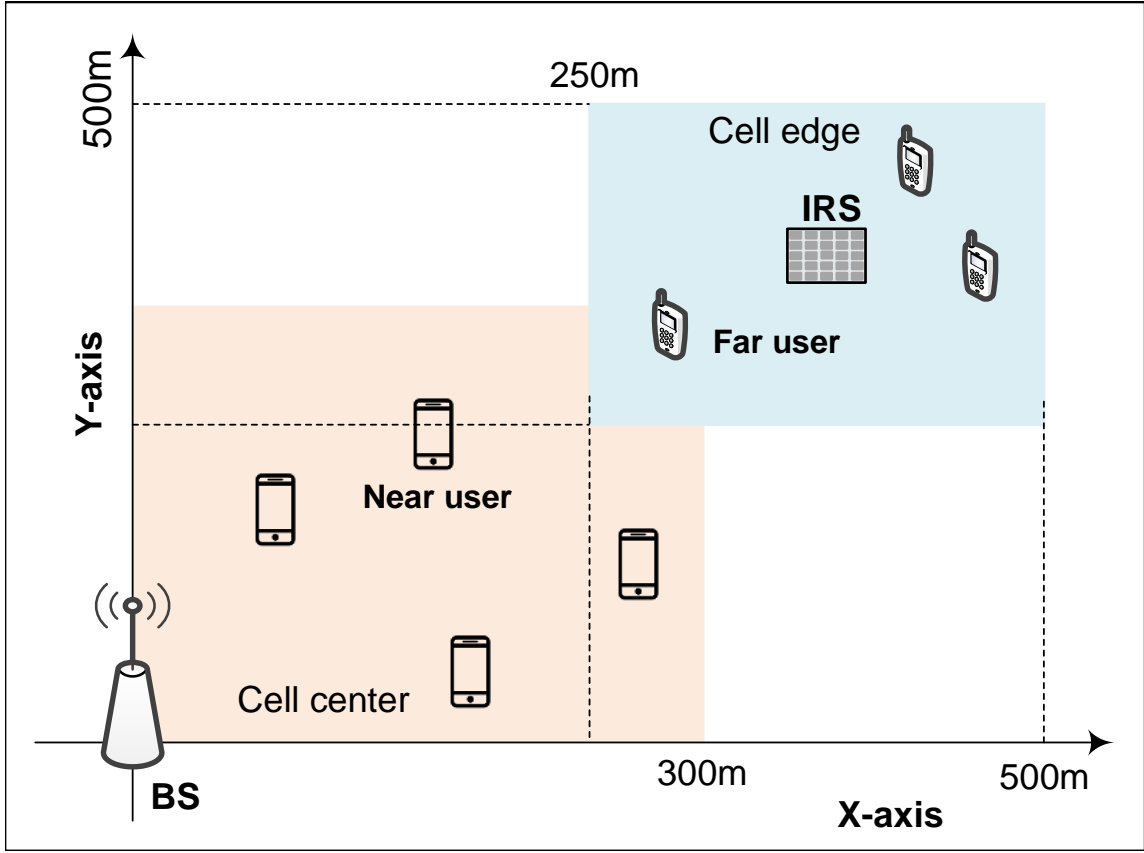
Fig. 2. Simulation scenario of a multi-user IRS system, where the cell coverage is comprised of a cell-center area and a cell-edge area.

LTE specification. We apply the formula $\sigma_n^2 = \kappa \cdot B_w \cdot T_0 \cdot N_f$ to compute the variance of AWGN, where κ is the Boltzmann constant, the temperature $T_0 = 290$Kelvin, and the noise figure $N_f = 9$dB.

The large-scale fading is computed by $\sigma^2 = 10^{\frac{\mathcal{P}+\mathcal{S}}{10}}$, where $\mathcal{P}$ is distance-dependent path loss, $\mathcal{S}$ stands for *log-normal* shadowing denoted by $\mathcal{S} \sim \mathcal{N}(0, \sigma_{sd}^2)$, and the standard derivation is generally set to $\sigma_{sd} = 8$dB. As [48], this paper employs the COST-Hata model to calculate $\mathcal{P}$, i.e.,

$$\mathcal{P} = \begin{cases} -\mathcal{P}_0 - 35\lg(d), & d > d_1 \\ -\mathcal{P}_0 - 15\lg(d_1) - 20\lg(d), & d_0 < d \leq d_1 \\ -\mathcal{P}_0 - 15\lg(d_1) - 20\lg(d_0), & d \leq d_0 \end{cases} \tag{26}$$

where d represents the propagation distance, d_0 and d_1 are reference points, which take values $d_0 = 10$m and $d_1 = 50$m, respectively. The first term is formulated as

$$\mathcal{P}_0 = 46.3 + 33.9\lg(f_0) - 13.82\lg(h_S) \tag{27}$$
$$- \Big[1.1\lg(f_0) - 0.7\Big]h_T + 1.56\lg(f_0) - 0.8,$$

which equals $\mathcal{P}_0 = 140.72$dB when the carrier frequency $f_0 = 1.9$GHz, the antenna height of BS or IRS $h_S = 15$m, and the UE antenna height $h_T = 1.65$m. In contrast, the path loss for the LOS channel between the BS and IRS can be computed through

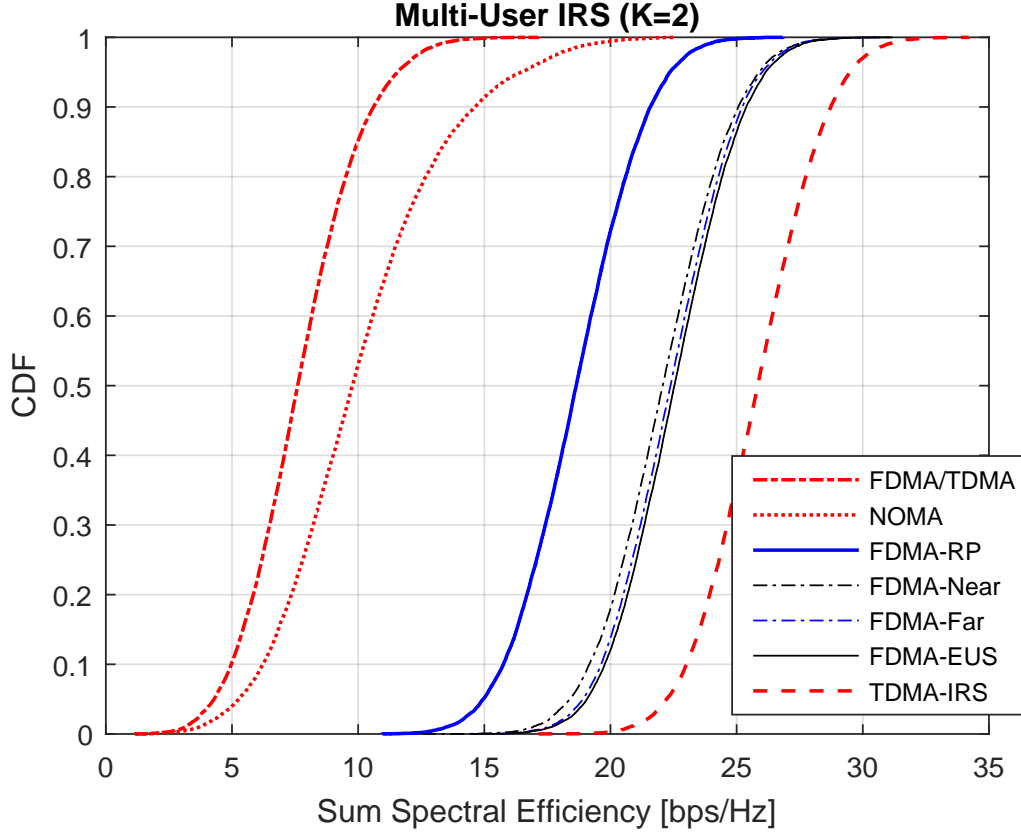$$L(d) = \frac{L_0}{d^{-\alpha}}, \tag{28}$$

Multi-User IRS (K=2)

Fig. 3. Performance comparisons of TDMA, NOMA and FDMA with different user scheduling and reflection optimization schemes in an IRS-aided multi-user MIMO systems: CDFs of the sum spectral efficiency with two users

where $L_0 = -30\,\text{dB}$ is the path loss measured at the reference distance of $1\,\text{m}$, $\alpha = 2$ means the free-space path loss exponent, and the Rician factor is set to $K = 5$.

For a comprehensive view, our evaluation compares different schemes and configurations as many as possible, including: 1) TDMA without the aid of IRS, where a radio frame is orthogonally divided into K time slots. At the kth slot, the BS sends the information symbol s_k to user k. The MRT $\mathbf{w}_k^\star = \mathbf{f}_k^*/\|\mathbf{f}_k\|$ is applied to achieve matched filtering in terms of the BS-UE direct link. 2) NOMA: the transmitter superimposes all information symbols into a single waveform as $\mathbf{s} = \sum_{k=1}^{K} \sqrt{\alpha_k} \mathbf{w}_k s_k$, where α_k represents the power allocation coefficient subjecting to $\sum_{k=1}^{K} \alpha_k \leqslant 1$. The optimal order of successive interference cancellation is detecting the user with the weakest channel gain first. Then, the corresponding component due to the weakest user is subtracted from the received signal at each user. In the second iteration, each user decodes the second weakest user using the residual signal. The cancellation iterates until each user gets its own symbol. 3) FDMA without the aid of IRS, where the BS applies the MRT $\mathbf{w}_k^\star = \mathbf{f}_k^*/\|\mathbf{f}_k\|$ to send the information symbol s_k at the kth subchannel. 4) TDMA in the IRS-aided system denoted by TDMA-IRS, where the IRS applies time-selective phase shifts at each slot. At the kth slot, alternating optimization is applied to jointly optimize active beamforming and passive reflection. 5) FDMA-RP means *randomly* setting the *phase* shifts of the surface in the IRS-aided FDMA system, and then each subchannel optimizes its own transmit vector $\mathbf{w}_k$ given the random but known reflection situation $\mathbf{\Theta}_r$. 6) FDMA-Near means using the CSI of the nearest user of the IRS to optimize the phase shifts, and then each subchannel optimizes its own transmit vector $\mathbf{w}_k$ in terms of the given reflection situation. 7) FDMA-Far
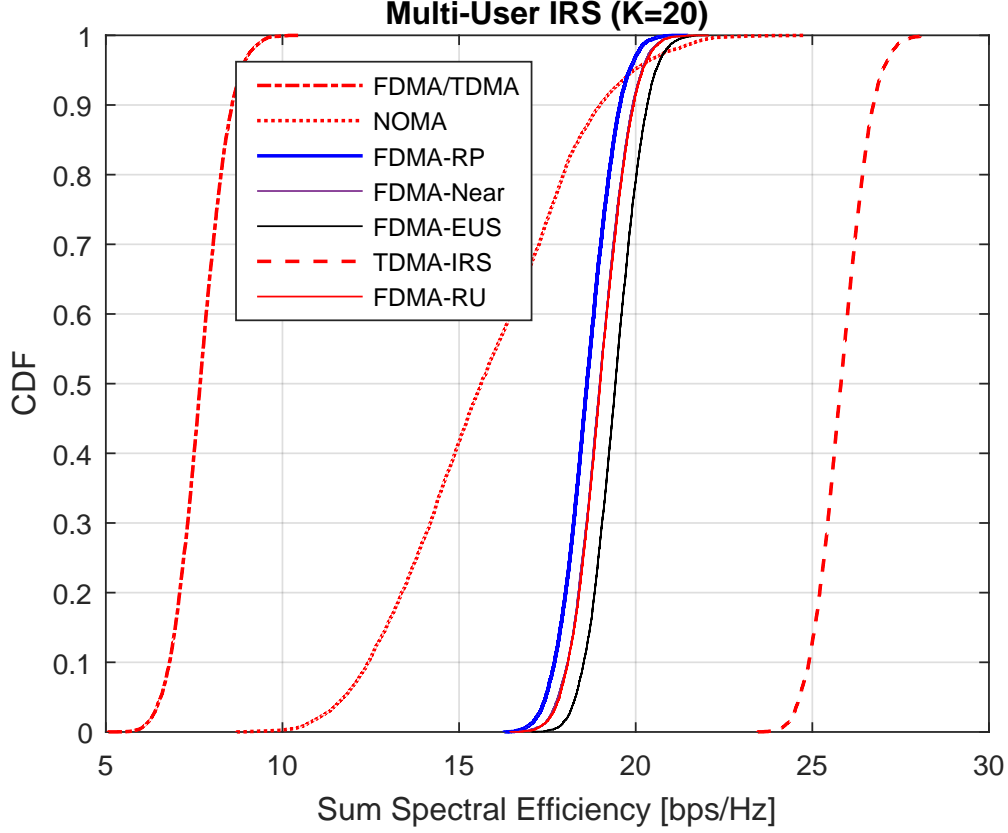
Fig. 4.   Performance comparisons of TDMA, NOMA and FDMA with different user scheduling and reflection optimization schemes in an IRS-aided multi-user MIMO systems: CDFs of the sum spectral efficiency with twenty users

means using the CSI of the farthest IRS user to optimize the phase shifts, and then each subchannel optimizes its own transmit vector in terms of the given reflection situation. 8) FDMA-EUS means exhaustive user selection to find the best user, which is selected for the reflection optimization, and then each subchannel optimizes its own transmit vector in terms of the given reflection situation. 9) FDMA-RU means randomly selecting a user for the reflection optimization, and then each subchannel optimizes its own transmit vector. It is observed in the simulations that three iterations are sufficient for the convergence of alternating optimization.

Fig.3 compares the cumulative distribution functions (CDFs) of the sum spectral efficiency in an IRS-aided multi-user MIMO system with $K = 2$ users, consisting of a far user and a near user. The conventional FDMA achieves the 95%-likely spectral efficiency (a common measure for cell-edge performance) of around $4.3\,\text{bps/Hz}$, and 50%-likely or median spectral efficiency of $7.6\,\text{bps/Hz}$. As expected, TDMA has the exactly same performance as FDMA in the absence of IRS. NOMA is superior to FDMA/TDMA due to the superposition of more users over the same time-frequency resource, where the 95%-likely and 50%-likely rates are increased to approximately $5.3\,\text{bps/Hz}$ and $9.7\,\text{bps/Hz}$, respectively. It is verified that the use of IRS brings substantial performance improvement. Even though random phase shifts are applied, the 95%-likely and 50%-likely rates of FDMA-RP grow to $15\,\text{bps/Hz}$ and $18.6\,\text{bps/Hz}$, respectively, amounting to almost three-fold improvement compared to FDMA without the aid of IRS. Due to exhaustive best-user searching and joint reflection optimization, FDMA-EUS further boosts the performance, reaching $19\,\text{bps/Hz}$ and $22.5\,\text{bps/Hz}$. Interestingly, selecting either a near or far user suffers from a slight rate

loss. That is to say, user scheduling does not provide a meaningful gain in the FDMA-IRS system. Compared with TDMA-IRS, achieving 95%-likely spectral efficiency of $22.18 \,\mathrm{bps/Hz}$ and 50%-likely spectral efficiency of $25.81 \,\mathrm{bps/Hz}$, there is a loss of approximately $3 \,\mathrm{bps/Hz}$. That is because the time-selective reflection optimally optimizes both users in TDMA-IRS, whereas one FDMA user suffers from phase-unaligned reflection due to the lack of frequency-selective reflection.

In addition, we also illustrate the performance comparison of these schemes in the case of $K = 20$ users. We observe that either random user scheduling or random phase reflection achieves the near-optimal performance, which has less than $1 \,\mathrm{bps/Hz}$ rate loss, in comparison with exhaustive user selection and optimal reflection optimization. That is because only one user gets the perfect performance with the aid of the IRS, whereas most of the users $(K - 1)$ suffer from un-aligned phase reflection. With the increasing number of users, the preference is random user selection and random phase shifts, which lowers the system complexity substantially but achieves the near-optimal performance.

V. Conclusions

This paper investigated multi-user scheduling and passive-beamforming optimization for (O)FDMA in a multi-user IRS communications system. For a comprehensive view, different user-scheduling strategies including exhaustive search, random search, farthest user, and nearest user, as well as different passive-beamforming methods, i.e., joint reflection optimization and random reflection, were presented. Theoretical analysis and numerical evaluation revealed a meaningful outcome. That is, FDMA-IRS does not need user scheduling when there are a few users. If the number of users becomes large, neither user scheduling nor reflection optimization is needed. This findings helps substantially simplifying the design of IRS-aided (O)FDMA communications systems (e.g., the estimation of cascaded channel is avoided) but achieve the near-optimal performance.

References

[1] T. Kaiser *et al.*, "Cognitive radio – a current snapshot and some thoughts on commercialization for future cellular systems," *J. Signal Process. Syst.*, vol. 73, no. 3, pp. 217–225, Dec. 2013.

[2] W. Jiang *et al.*, "Key issues towards beyond LTE-Advanced systems with cognitive radio," in *Proc. IEEE 2013 Workshop on Sign. Proc. Adv. in Wireless Commun. (SPAWC)*, Darmstadt, Germany, Jun. 2013, pp. 510–514.

[3] H. Cao *et al.*, "The design of an LTE-A system enhanced with cognitive radio," in *Proc. Eur. Signal Process. Conf. (EUSIPCO)*, Marrakech, Morocco, Sep. 2013, pp. 1–6.

[4] M. D. Mueck *et al.*, "Novel spectrum usage paradigms for 5G," White Paper, IEEE Technical Committee on Cognitive Networks (TCCN) Special Interest Group on *Cognitive Radio for 5G*, Nov. 2014.

[5] J. P. Santos *et al.*, "SELFNET framework self-healing capabilities for 5G mobile networks," *Trans. Emerg. Telecommu. Techno.*, vol. 27, no. 9, pp. 1225–1232, Sep. 2016.

[6] P. Neves *et al.*, "The SELFNET approach for autonomic management in an NFV/SDN networking paradigm," *Int. J. Distrib. Sensor Netw.*, pp. 1–17, Feb. 2016.

[7] W. Jiang *et al.*, "Experimental results for Artificial Intelligence-based self-organized 5G networks," in *Proc. IEEE Int. Symp. on Pers., Indoor and Mobile Radio Commun. (PIMRC)*, Montreal, Canada, Oct. 2017.

[8] ——, "Intelligent network management for 5G systems: The SELFNET approach," in *Proc. IEEE Eur. Conf. on Netw. and Commun. (EUCNC)*, Oulu, Finland, Jun. 2017, pp. 109–113.

[9] ——, "Autonomic network management for software-define and virtualized 5G systems," in *Proc. Eur. Wireless*, Dresden, Germany, May 2017.

[10] W. Jiang, "Device-to-device based cooperative relaying for 5G network: A comparative review," *ZTE Communications*, vol. 15, pp. 60–66, Jun. 2017.

[11] W. Jiang *et al.*, "A SON decision-making framework for intelligent management in 5G mobile networks," in *Proc. IEEE Int. Conf. on Compu. and Commun. (ICCC)*, Chengdu, China, Dec. 2017.

[12] ——, "An SDN/NFV proof-of-concept test-bed for machine learning-based network management," in *Proc. IEEE Int. Conf. on Compu. and Commun. (ICCC)*, Chengdu, China, Dec. 2018.

[13] W. Jiang, M. Strufe, and H. Schotten, "Machine learning-based framework for autonomous network management in 5G systems," in *Proc. 2018 Eur. Conf. on Netw. and Commun. (EuCNC)*, Ljubljana, Slovenia, Jun. 2018.

[14] W. Jiang, S. D. Anton, and H. D. Schotten, "Intelligence slicing: A unifed framework to integrate artificial intelligence into 5G networks," in *Proc. 2019 12th IFIP Wireless and Mobile Netw. Conf. (WMNC)*, Paris, France, Sep. 2019, pp. 227–232.

[15] W. Jiang and F.-L. Luo, "Editorial: Special topic on computational radio intelligence: One key for 6G wireless," *ZTE Communications*, vol. 17, no. 4, pp. 1–3, Dec. 2019.

[16] W. Jiang *et al.*, "The road towards 6G: A comprehensive survey," *IEEE Open J. Commun. Society*, vol. 2, pp. 334–366, Feb. 2021.

[17] W. Jiang and H. D. Schotten, "The kick-off of 6G research worldwide: An overview," in *Proc. 2021 Seventh IEEE Int. Conf. on Comput. and Commun. (ICCC)*, Chengdu, China, Dec. 2021.

[18] W. Jiang and F.-L. Luo, *6G Key Technologies: A Comprehensive Guide.* New York, USA: IEEE Press & Wiley, 2023.

[19] W. Jiang and H. Schotten, "Neural network-based fading channel prediction: A comprehensive overview," *IEEE Access*, vol. 7, pp. 118 112–118 124, Aug. 2019.

[20] W. Jiang and H. D. Schotten, "Deep learning for fading channel prediction," *IEEE Open J. the Commun. Society*, vol. 1, pp. 320–332, Mar. 2020.

[21] ——, "Multi-antenna fading channel prediction empowered by artificial intelligence," in *Proc. 2018 IEEE Veh. Technol. Conf. (VTC-Fall)*, Chicago, USA, Aug. 2018.

[22] W. Jiang and H. Schotten, "Neural network-based channel prediction and its performance in multi-antenna systems," in *Proc. 2018 IEEE Veh. Technol. Conf. (VTC-Fall)*, Chicago, USA, Aug. 2018.

[23] W. Jiang and H. D. Schotten, "A comparison of wireless channel predictors: Artificial Intelligence versus Kalman filter," in *Proc. 2019 IEEE Int. Commun. Conf. (ICC)*, Shanghai, China, May 2019.

[24] W. Jiang and H. Schotten, "Recurrent neural network-based frequency-domain channel prediction for wideband communications," in *Proc. 2019 IEEE Veh. Technol. Conf. (VTC-Spring)*, Kuala Lumpur, Malaysia, Apr. 2019.

[25] W. Jiang, M. Strufe, and H. Schotten, "Long-range fading channel prediction using recurrent neural network," in *Proc. 2020 IEEE Consum. Commun. and Netw. Conf.*, Las Vegas, USA, Jan. 2020.

[26] W. Jiang and H. D. Schotten, "A deep learning method to predict fading channel in multi-antenna systems," in *Proc. 2020 IEEE Veh. Technol. Conf. (VTC-Spring)*, Antwerp, Belgium, May 2020.

[27] ——, "Recurrent neural networks with long short-term memory for fading channel prediction," in *Proc. 2020 IEEE Veh. Technol. Conf. (VTC-Spring)*, Antwerp, Belgium, May 2020.

[28] W. Jiang, H. Schotten, and J.-Y. Xiang, "Neural network based wireless channel prediction," in *Machine Learning for Future Wireless Communications*, F. L. Luo, Ed. United Kindom: John Wiley&Sons and IEEE Press, 2020, ch. 16.

[29] A. M. Seid *et al.*, "Multi-agent DRL for task offloading and resource allocation in multi-UAV enabled IoT edge network," *IEEE Trans. Netw. Serv. Manag.*, vol. 18, no. 4, pp. 4531 – 4547, Dec. 2021.

[30] G. Sun *et al.*, "Dynamic resource reservation for ultra-low latency IoT air-interface slice," *KSII Trans. Internet Info. Syst.*, vol. 11, no. 7, pp. 3309–3328, Jun. 2017.

[31] ——, "Dynamic reservation and deep reinforcement learning based autonomous resource slicing for virtualized radio access networks," *IEEE Access*, vol. 7, pp. 45 758–45 772, Apr. 2019.

[32] ——, "Resource slicing and customization in ran with dueling deep q-network," *J. Netw. Computer App.*, vol. 157, May 2020.

[33] ——, "Autonomous resource slicing for virtualized vehicular networks with d2d communications based on deep reinforcement learning," *IEEE Syst. J.*, vol. 14, no. 4, pp. 4694–4705, Dec. 2020.

[34] ——, "Autonomous resource provisioning and resource customization for mixed traffics in virtualized radio access network," *IEEE Syst. J.*, vol. 13, no. 3, pp. 2454 – 2465, Sep. 2019.

[35] ——, "Transfer learning for autonomous cell activation based on relational reinforcement learning with adaptive reward," *IEEE Syst. J.*, vol. 16, no. 1, pp. 1044 – 1055, Mar. 2021.

[36] Y. H. Yacob *et al.*, "An optimal incentive mechanism for blockchain-enabled content caching in device-to-device communication," in *Proc. 2022 IEEE Int. Conf. Computing, Commun., Perception Quantum Techno. (CCPQT 2022)*, Xiamen, China, Aug. 2022.

[37] H. Cao *et al.*, "A robust radio access technology classification scheme with practical considerations," in *Proc. IEEE Int. Symp. on Pers., Indoor and Mobile Radio Commun. (PIMRC)*, London, UK, Sep. 2013, pp. 36–40.

[38] H. cao *et al.*, "Multi-channel robust spectrum sensing with low-complexity filter bank realization," in *Proc. IEEE Int. Symp. on Pers., Indoor and Mobile Radio Commun. (PIMRC)*, London, UK, Sep. 2013, pp. 861–865.

[39] H. Cao, W. Jiang, and T. Kaiser, "Parallel in-band signal detection with self-interference suppression for cognitive LTE," in *Proc. 2014 IEEE Wireless Commun. and Netw. Conf. (WCNC)*, Istanbul, Turkey, Apr. 2014.

[40] W. Jiang, D. Yu, and Y. Ma, "A tracking algorithm in RFID reader network," in *Proc. 2006 Japan-China Joint Workshop on Frontier of Compu. Sci. and Techno. (FCST)*, Fukushima, Japan, Nov. 2006, pp. 164–171.

[41] W. Jiang and Y. Ma, "Interference analysis of microwave RFID and 802.11b WLAN," in *Proc. 2007 Int. Conf. on Wireless Commun., Netw. and Mobile Computing (WiCOM)*, Shanghai, China, Sep. 2007, pp. 2062–2065.

[42] W. Jiang, "Bit error rate analysis of Wi-Fi and bluetooth under the interference of 2.45GHz RFID," *J. China Universities of Posts and Telecommun.*, vol. 14, pp. 89–93, Oct. 2007.

[43] W. Jiang and H. D. Schotten, "Initial beamforming for millimeter-wave and terahertz communications in 6G mobile systems," in *Proc. 2022 IEEE Wireless Commun. and Netw. Conf. (WCNC)*, Austin, USA, Apr. 2022.

[44] ——, "Initial access for millimeter-wave and terahertz communications with hybrid beamforming," in *Proc. 2022 IEEE Int. Commun. Conf. (ICC)*, Seoul, South Korea, May 2022.

[45] W. Jiang and H. Schotten, "Dual-beam intelligent reflecting surface for millimeter and THz communications," in *Proc. 2022 IEEE 95th Veh. Techno. Conf. (VTC2022-Spring)*, Helsinki, Finland, Jun. 2022.

[46] G. Yuan *et al.*, "Bidirectional branch and bound based antenna selection in massive MIMO systems," in *Proc. 2015 IEEE 23rd Int. Symp. on Pers., Indoor and Mobile Radio Commun. (PIMRC)*, Hongkong, China, Sep. 2015, pp. 563 – 568.

[47] W. Jiang and Y. Wang, "User pairing method, device and system for realizing user scheduling," U.S. Patent 10 212 723, Feb. 19, 2019.

[48] W. Jiang and H. D. Schotten, "Cell-free massive MIMO-OFDM transmission over frequency-selective fading channels," *IEEE Commun. Lett.*, vol. 25, no. 8, pp. 2718 – 2722, Aug. 2021.

[49] W. Jiang and H. Schotten, "Impact of channel aging on zero-forcing precoding in cell-free massive MIMO systems," *IEEE Commun. Lett.*, vol. 25, no. 9, pp. 3114 – 3118, Sep. 2021.

[50] ——, "Opportunistic AP selection in cell-free massive MIMO-OFDM systems," in *Proc. 2022 IEEE 95th Veh. Techno. Conf. (VTC2022-Spring)*, Helsinki, Finland, Jun. 2022.

[51] ——, "Deep learning-aided delay-tolerant zero-forcing precoding in cell-free massive MIMO," in *Proc. 2022 IEEE 96th Veh. Techno. Conf. (VTC2022-Fall)*, London, UK, Sep. 2022.

[52] M. D. Renzo *et al.*, "Smart radio environments empowered by reconfigurable intelligent surfaces: How it works, state of research, and the road ahead," *IEEE J. Sel. Areas Commun.*, vol. 38, no. 11, pp. 2450 – 2525, Nov. 2020.

[53] W. Jiang and H. Schotten, "Multi-user reconfigurable intelligent surface-aided communications under discrete phase shifts," in *Proc. 36th IEEE Int. Workshop on Commun. Qual. and Reliability (CQR 2022)*, Arlington, United States, Sep. 2022.

[54] ——, "Intelligent reflecting vehicle surface: A novel IRS paradigm for moving vehicular networks," in *Proc. 2022 IEEE 40th Military Commun. Conf. (MILCOM 2022)*, Rockville, MA, USA, Nov. 2022.

[55] ——, "Performance impact of channel aging and phase noise on intelligent reflecting surface," *IEEE Commun. Lett.*, vol. 27, no. 1, pp. 347–351, Jan. 2023.

[56] ——, "Orthogonal and non-orthogonal multiple access for intelligent reflection surface in 6G systems," in *Proc. 2023 IEEE Wireless Commun. and Netw. Conf. (WCNC)*, Glasgow, Scotland, UK, Mar. 2023.

[57] W. Jiang and H. D. Schotten, "Capacity analysis and rate maximization design in RIS-aided uplink multi-user MIMO," in *Proc. 2023 IEEE Wireless Commun. and Netw. Conf. (WCNC)*, Glasgow, Scotland, UK, Mar. 2023.

[58] Q. Wu and R. Zhang, "Intelligent reflecting surface enhanced wireless network via joint active and passive beamforming," *IEEE Trans. Wireless Commun.*, vol. 18, no. 11, pp. 5394 – 5409, Nov. 2019.

[59] M. D. Renzo *et al.*, "Reconfigurable intelligent surfaces vs. relaying: Differences, similarities, and performance comparison," *IEEE Open J. Commun. Society*, vol. 1, pp. 798 – 807, Jun. 2020.

[60] Z. Wang, L. Liu, and S. Cui, "Channel estimation for intelligent reflecting surface assisted multiuser communications: Framework, algorithms, and analysis," *IEEE Trans. Wireless Commun.*, vol. 19, no. 10, pp. 6607 – 6620, Oct. 2020.

[61] K. Zhi *et al.*, "Uplink achievable rate of intelligent reflecting surface-aided millimeter-wave communications with low-resolution ADC and phase noise," *IEEE Wireless Commun. Lett.*, vol. 10, no. 3, pp. 654 – 658, Mar. 2021.

[62] B. Zheng and R. Zhang, "Intelligent reflecting surface-enhanced OFDM: Channel estimation and reflection optimization," *IEEE Wireless Commun. Lett.*, vol. 9, no. 4, pp. 518 – 522, Apr. 2020.

[63] S. Hu, F. Rusek, and O. Edfors, "Beyond massive MIMO: The potential of data transmission with large intelligent surfaces," *IEEE Trans. Signal Process.*, vol. 66, no. 10, pp. 2746 – 2758, May 2018.

[64] B. Di *et al.*, "Hybrid beamforming for reconfigurable intelligent surface based multi-user communications: Achievable rates with limited discrete phase shifts," *IEEE J. Sel. Areas Commun.*, vol. 38, no. 8, pp. 1809 – 1822, Aug. 2020.

[65] W. Jiang and T. Kaiser, "From OFDM to FBMC: Principles and Comparisons," in *Signal Processing for 5G: Algorithms and Implementations*, F. L. Luo and C. Zhang, Eds. United Kindom: John Wiley&Sons and IEEE Press, 2016, ch. 3.

[66] B. Zheng, Q. Wu, and R. Zhang, "Intelligent reflecting surface-assisted multiple access with user pairing: NOMA or OMA?" *IEEE Commun. Lett.*, vol. 24, no. 4, pp. 753 – 757, Apr. 2020.

[67] Y. Chen *et al.*, "Toward the standardization of non-orthogonal multiple access for next generation wireless networks," *IEEE Commun. Mag.*, vol. 56, no. 3, pp. 19 – 27, Mar. 2018.

[68] Z. Chu *et al.*, "Resource allocation for IRS-assisted wireless-powered FDMA IoT networks," *IEEE Internet of Things J.*, vol. 9, no. 11, pp. 8774 – 8785, Jun. 2022.

[69] W. Jiang, H. Cao, and T. Kaiser, "Opportunistic space-time coding to exploit cooperative diversity in fast-fading channels," in *Proc. 2014 IEEE Int. Commun. Conf. (ICC)*, Sydney, NSW, Australia, Jun. 2014, pp. 4814–4819.

[70] W. Jiang *et al.*, "Opportunistic relaying over aerial-to-terrestrial and device-to-device radio channels," in *Proc. 2014 IEEE Intl. Conf. on Commun. (ICC)*, Sydney, Australia, Jul. 2014, pp. 206–211.

[71] ——, "Achieving high reliability in aerial-terrestrial networks: Opportunistic space-time coding," in *Proc. IEEE Eur. Conf. on Net. and Commun. (EUCNC)*, Bologne, Italy, Jun. 2014.

[72] W. Jiang, H. Cao, and T. Kaiser, "An MGF-based performance analysis of opportunistic relay selection with outdated CSI," in *Proc. 2014 IEEE 79th Veh. Technol. Conf. (VTC-Spring)*, Seoul, South Korea, May 2014.

[73] ——, "Analysis of generalized selection combining in cooperative networks with outdated CSI," in *Proc. 2014 IEEE Wireless Commun. and Netw. Conf. (WCNC)*, Istanbul, Turkey, Apr. 2014.

[74] ——, "Power optimal allocation in decode-and-forward opportunistic relaying," in *Proc. 2014 IEEE Wireless Commun. and Netw. Conf. (WCNC)*, Istanbul, Turkey, Apr. 2014.

[75] W. Jiang, T. Kaiser, and A. J. H. Vinck, "A robust opportunistic relaying strategy for co-operative wireless communications," *IEEE Trans. Wireless Commun.*, vol. 15, no. 4, pp. 2642–2655, Apr. 2016.

[76] W. Jiang and H. Schotten, "Predictive relay selection: A cooperative diversity scheme using deep learning," in *Proc. 2021 IEEE Wireless Commun. and Netw. Conf. (WCNC)*, Nanjing, China, Mar. 2021.

[77] W. Jiang and H. D. Schotten, "A simple cooperative diversity method based on deep-learning-aided relay selection," *IEEE Trans. Veh. Technol.*, vol. 70, no. 5, pp. 4485 – 4500, May 2021.

[78] W. Jiang and Z. Zhao, "Low-complexity spectral precoding for rectangularly pulsed OFDM," in *Proc. 2012 IEEE Veh. Technol. Conf. (VTC-Fall)*, Quebec City, QC, Canada, Sep. 2012.

[79] W. Jiang and M. Schellmann, "Suppressing the out-of-band power radiation in multi-carrier systems: A comparative study," in *Proc. 2012 IEEE Global Commun. Conf. (Globecom)*, Anaheim, CA, USA, Dec. 2012, pp. 1477 – 1482.

[80] W. Jiang, "Multicarrier transmission schemes in cognitive radio," in *Proc. 2012 Int. Symp. on Signals, Syst., and Electron. (ISSSE)*, Potsdam, Germany, Oct. 2012.

[81] G. Sun, X. Zhou, and W. Jiang, "Method and apparatus for sending signals," U.S. Patent 9 031 155, May 12, 2015.

[82] G. Sun, W. Jiang, and G. Zhao, "Method for reducing inter-femtocell interference and femtocell base station," U.S. Patent 9 369 244, Jun. 14, 2016.

[83] W. Jiang, "Method for dynamically setting virtual subcarriers, receiving method, apparatus and system," U.S. Patent 9 319 885, Apr. 19, 2016.

[84] Q. Wu and R. Zhang, "Beamforming optimization for wireless network aided by intelligent reflecting surface with discrete phase shifts," *IEEE Trans. Commun.*, vol. 68, no. 3, pp. 838 – 1851, Mar. 2020.

[85] X. Yang, W. Jiang, and B. Vucetic, "A random beamforming technique for omnidirectional coverage in multiple-antenna systems," *IEEE Trans. Veh. Technol.*, vol. 62, no. 3, pp. 1420 – 1425, Mar. 2013.

[86] W. Jiang and X. Yang, "Method and apparatus for transmitting broadcast signal," U.S. Patent Application 13/685 426, Nov. 26, 2012.

[87] X. Yang, W. Jiang, and B. Vucetic, "A random beamforming technique for broadcast channels in multiple antenna systems," in *Proc. 2011 IEEE Veh. Techno. Conf. (VTC Fall)*, San Francisco, USA, Sep. 2011.

[88] X. Yang and W. Jiang, "Method and apparatus for cell/sector coverage of a public channel through multiple antennas," U.S. Patent 8 537 785, Sep. 17, 2013.

[89] ——, "Method, apparatus, and system for controlling multi-antenna signal transmission," U.S. Patent Application 13/654 743, Oct. 18, 2012.

[90] W. Jiang and X. Yang, "An enhanced random beamforming scheme for signal broadcasting in multi-antenna systems," in *Proc. 2012 IEEE 23rd Int. Symp. on Pers., Indoor and Mobile Radio Commun. (PIMRC)*, Sydney, NSW, Australia, Sep. 2012, pp. 2055 – 2060.

[91] X. Yang and W. Jiang, "Method and apparatus for transmitting signals in a multiple antennas system," U.S. Patent 8 170 132, May 1, 2012.